doi:10.4149/neo_2011_06_538

Plasmid-based STAT3-siRNA efficiently inhibits breast tumor growth and metastasis in mice

L. DAI[1], L. CHENG[1], X. ZHANG[1], Q. JIANG[1,2], S. ZHANG[1], S. WANG[1], Y. LI[1], X. CHEN[1], T. DU[1], Y. YANG[1], H. TIAN[1], P. FAN[1], N. YAN[1], L. DAI[1], Y. WEI[1], H. DENG[1*]

[1]State Key Laboratory of Biotherapy, West China Hospital, Sichuan University, Ke-yuan Road 4, No. 1, Gao-peng Street, Chengdu, Sichuan, 610041, the People's Republic of China; [2]Sichuan Provincial Hospital for Women and Children, Chengdu, Sichuan, 610041, the People's Republic of China

**Correspondence: denghongx@scu.edu.cn*

Received May 26, 2011

Signal transducer and activator of transcription 3 (STAT3) plays an important role in the tumor formation and metastasis. In this study, short hairpin RNA targeting STAT3 was cloned into pGenesil-2 plasmid vector and the effects of STAT3 silencing in 4T1 breast cancer cells were analyzed both *in vitro* and *in vivo*. Forty-eight hours after transfecting with pSi-STAT3, the expression level of STAT3, the upstream regulator and downstream targets were measured using Western blot. Moreover, the effects of pSi-STAT3 on migration and invasion in 4T1 cells were tested using wound-healing and tube formation assay. Furthermore, 4T1 subcutaneous mice model was used to evaluate the effects of pSi-STAT3 on tumor growth and metastasis. Proliferation, apoptosis, angiogenesis in tumor tissues and lung metastases were measured by PCNA, TUNEL, and CD31 immunostaining, respectively. Our results indicated that siRNA targeting STAT3 could significantly silence STAT3 expression in 4T1 breast cancer cells and result in inhibition of 4T1 breast cells migration and HUVECs tube formation. *In vivo*, pSi-STAT3 delayed tumor growth ($p<0.01$) and reduced tumor weight ($p<0.01$) by 67.19% and lung metastases ($p<0.01$) by 86.81% compared with the 5% GS control group, accompanied with apoptosis induction ($p<0.01$) and angiogenesis inhibition ($p<0.01$). In summary, our data showed that knockdown of STAT3 by plasmid-based siRNA might be a potential therapy against breast cancer.

Key words: STAT3, RNA interference, breast cancer, metastasis

Surgery, radiation therapy and chemotherapy are the useful way to control many primary tumors, but these treatments have limited effectiveness in curbing the metastases formed by disseminated primary tumor cells at distant anatomic sites (1). And these metastases caused ninety percent of cancer-related mortality (2). Breast cancer is the major cause of morbidity and mortality in women worldwide, meanwhile lung metastases are occurred in most breast cancer (3). There are abundant studies to show that constitutive activated signal transducer and activator of transcription 3 (STAT3) is frequently found in breast cancer samples (4).

STAT3 is a point of convergence for numerous oncogenic signaling pathways, including tumor cell apoptosis, cell cycle, cell invasion and tumor angiogenesis. There are abundant evidences for the involvement of STAT3 in tumor cell invasion. Specifically, activated STAT3 regulates the invasion of melanoma cells by regulating the gene transcription of matrix metalloproteinase 2 (MMP-2) and matrix metalloproteinase 9 (MMP-9) (5), which play an important role in the process of invasion and metastasis of many malignant tumors, particularly because of its ability to degrade the basement membrane (6). Recent studies have shown that STAT3 transcriptionally activates Twist (7), a transcription factor that control embryonic morphogenesis and imparts carcinoma cells the ability to metastasize from the mammary gland to the lung (8). Activated STAT3 affects tumor angiogenesis by regulating the expression of multiple pro-angiogenic molecules in tumor cells and participating in the signal transduction of angiogenic molecule receptors in tumor endothelial cells. In fact, STAT3 activation is necessary for endothelial cell proliferation, migration, and microvascular tube formation, by directly target VEGF and bFGF (5, 9, 10). There is tight association between STAT3 activation and tumor progres-

sion. Thus, STAT3 is an attractive molecular target for the development of novel cancer therapeutics.

RNA interference (RNAi) is a specific posttranscriptional gene silencing mechanism, which is triggered by double-stranded RNA (dsRNA) and regulates the expression of protein-coding genes (11). Since its high efficacy and specificity in antiproliferative and/or proapoptotic effects in cell-culture systems or in preclinical animal models, RNA interference technology is now widely used as a potential therapeutic strategy (12). Several siRNA have been into the clinic, including Bevasiranib (Acuity Pharmaceuticals, Philadelphia, Pennsylvania, USA) which tested in human clinical trial; RTP801i-14(Quark Pharmaceuticals, Fremont, California, USA) is now running a phase I/IIA clinical trial (13).

The 4T1 cell line was originally derived from a spontaneous mouse mammary carcinoma from the BALB/c strain (14). It has been reported that 4T1 cells get the high capacity of migration and invasion (15). The injection of 4T1 cells into the subcutaneous of the BALB/c mice could form metastases at the distant organs relatively primary tumor growth (16). Therefore, 4T1 breast subcutaneous mice model is an appropriate model to mimic human breast cancer with regard to tumor growth and metastasis *in vivo*. Thus, it is the best mice model to investigate the effect of STAT3 on primary tumor growth and metastasis.

In this study, we specifically silenced STAT3 using a plasmid-based siRNA expression system and studied the effects on breast cancer cell growth and metastasis *in vitro* and *in vivo*. The results shown that pSi-STAT3 significantly inhibit tumor growth and metastasis *in vivo*.

Materials and methods

Vector construction. Plasmids were constructed by using the pGensil-2 parental vector (Genesil Biotechnology Company, Wuhan, China). Oligonucleotide sequences of STAT3-siRNA (5'-CAG GGT GTC AGA TCA CAT GGG CTA A-3') were designed according to a published sequence of STAT3-siRNA (17), which was shown to efficiently silence STAT3 expression *in vitro* and *in vivo*. Oligonucleotide sequences of scramble-siRNA, which have no homology with any of the mammalian sequence, were designed as negative. SiRNA-expressing plasmids were constructed by the Genesil Biotechnology Company (Wuhan, China). The resulting recombinant plasmid was named as pSi-STAT3 or pSi-Scramble, respectively. Both of the two constructs were verified by DNA sequencing. Plasmids were extracted using EndoFree Plasmid Giga kits (Qiagen GmbH, Hilden, Germany) from DH5α *Escherichia coli* transformants and stored at –20 °C before use. The concentration was determined by measuring A_{260} /A_{280} ratio using UV spectorphotometry.

Cell line and transfection conditions. The 4T1 cell line was obtained from American Type Culture Collection (ATCC, Manassas, VA, USA). 4T1 cells were cultured in Dulbecco's Modified Eagle's Medium containing 10 % FBS (Gibco, Carlsbad, CA, USA). All the cells were maintained in a humidified atmosphere containing 5 % CO_2 at 37 °C. Cell transfection was carried out using FuGENE® HD Transfection Reagent (Roche, Indianapolis, IN, USA) according to the manufacturer's instructions. Briefly, 4T1 cells were seeded in 6-well plates at a density of 2×10^5 cells/well and cultured for 24 h to reach 70~80% confluence. 2 μg plasmids (pSi-Scramble or pSi-STAT3) were diluted in 100 μl media without serum and added 5 μl FuGENE® HD Transfection Reagent to the tubes containing diluted DNA, mixed and incubated the transfection complex for 15 min at room temperature, and then added to the 6-well dishes. Meanwhile, medium alone was used as blank agent. Cells and the supernatant were harvested 48 h after transfection for RT-PCR, Western blot and human umbilical vein endothelial cells (HUVECs) tube formation analysis. All transfections were performed in triplicate.

Western blot. Cells were lysed on ice for 30 min with RIPA Lysis Buffer (containing 50 mM Tris-HCl, pH 7.4; 1 % NP-40; 0.25 % Na-deoxycholate; 150 mM NaCl; 1 mM EDTA; 1 mM PMSF; 1 μg/ml aprotinin, leupeptin, pepstatin each; 1 mM Na3VO4; 1 mM NaF). The proteins (10 μg) were separated by SDS-polyacrylamide gel electrophoresis (SDS-PAGE) and electronically transferred onto a polyvinylidene difluoride membrane (Millipore, Bedford, MA). After blocking, the membranes were incubated with recommended dilution primary antibodies against STAT3, p-53, Cyclin D1, Src, pTyr-Src, AKT, pSer-AKT, Survivin, MMP-9 and MMP-2 (Cell Signaling, Boston, MA, USA), VEGF and GAPDH (Santa Cruz Biotechnology, Santa Cruz, CA, USA), followed by incubation with peroxidase conjugated secondary antibodies (Abcam, Cambridge, MA, USA). Peroxidase-labeled bands were visualized using an ECL kit (Pierce, Rockford, IL, USA).

Cell proliferation assay. 4T1 cells were plated out in 200 μl of medium at a concentration of 1×10^4 cells per well in 96-well plate. 3-(4,5-dimethylthiazol-2-yl) -2,5-diphenyltetrazolium (MTT) (Sigma, Poole, Dorset, England) was dissolved in H_2O, and 100 μl was added into the 96-well plate. MTT-formazan produced by cells was obtained by incubation of cells for 4 hours. MTT was removed and the formazan crystals dissolved in DMSO. The absorbance was determined at wavelength of 570 nm. The same experiments were performed in three times.

Tube formation assay. The wells of a 96-well plate were coated with ice-cold BD MatrigelTM matrix gel solution (BD Biosciences, San Jose, CA, USA). After polymerizing the matrix at 37 °C, HUVECs were seeded onto the polymerized EC matrix at a concentration of 2×10^4 cells in 100 μl of EGM-2 (Lonza Walkersville, Walkersville, MD, USA) media per well; 100 μl of the cell supernatant after transfection 48 h was immediately added. The tubule branches were photographed after 6 h of incubation. The HUVECs capillary-like structures were counted in per yield. The results of three independent experiments are given.

Wound-healing assay. 4T1 cells were grown to 80–90% confluence in 6-well plates, which were transfected by STAT3-siRNA. A wound was made by dragging a plastic pipette tip across the cell surface after 24 h. The phase contrast images of the wounds were recorded at 37°C for incubations of 0 and 48 h, and 3 separate experiments were performed. The cells were transfected by pSi-Scramble or blank as the controls. Image J software was used to evaluate the migration rate of 4T1 cells.

Cationic liposome and preparation of pDNA/lipoplexes. Cationic liposome was prepared as multilamellar vesicles for in vivo use as described previously. Briefly, DOTAP (1, 2 dioleoyl-3-trimethylammonium-propoane) (Alabaster, AL, USA) and cholesterol (Sigma-Aldrich, St. Louis, MO) were mixed in a 1:1 molar ratio, dried down in round-bottom tubes, then rehydrated in 5 % glucose solution by heating at 50 °C for 6 h. For *in vivo* injection, pDNA/lipoplexes were prepared immediately before injection by gently mixing cationic liposome with plasmid DNA at a ratio of 12.5 μg total cationic liposome to 2.5 μg plasmid DNA, to a final concentration of 12.5 μg plasmid DNA per ml in a sterile solution of 5 % glucose in water.

Tumor growth and treatments in vivo. To establish 4T1 subcutaneous cancer model, 8×10^5 4T1 cells were injected subcutaneously into the right flank regions of female BALB/c mice (6-8 weeks old). After a week, when the tumors could be palpable, the animals were randomly assigned to three independent groups of five mice and subjected to systemic treatment with one of the following treatments: 5 % glucose, pSi-Scramble, and pSi-STAT3. Plasmid DNA (2.5 μg) and cationic liposome (12.5 μg), in 100 μl of 5 % glucose was injected into the mouse tail vein three times a week (on Monday, Wednesday, and Friday). Tumor diameters were measured one time every three days during the treatment period. Tumor volume was estimated using the formula: tumor volume (mm^3) = length (mm) × [width (mm)]^2 × 1/ 2. The weight, appetite, and behavior of the mice were observed. Mice were euthanized after 10 times of treatment and dissected tumors were weighed. The tumors and viscera were examined grossly and microscopically stained with H&E. Animal studies were performed in accordance with the Institutional Animal Care and Treatment Committee of Sichuan University (Chengdu, People's Republic of China).

Immunostaining and H&E staining. Expression of STAT3, VEGF, PCNA and CD31 was performed with rabbit anti-mouse STAT3 antibody (Cell Signaling, Boston, MA , USA), rabbit anti-mouse VEGF antibody, mouse anti-human PCNA antibody (Santa Cruz Biotechnology, Santa Cruz, CA, USA), and rat anti-mouse CD31 antibody (BD Biosciences, San Jose, CA, USA), respectively. Tumor sections (3-5 μm) of paraffin-embedded were mounted on 3-aminopropyl triethoxysilane (APES)-coated glass slides. Sections were deparaffinized in xylene, treated with a graded series of alcohol [100 %, 95 %, and 80 % ethanol/double-distilled H_2O (v/v)], and rehydrated in PBS (pH 7.4). Antigene retrieval was done by heating for 3 min in a pressure cooker with 0.1 mol/L citrate buffer (pH 6.0). Endogenous peroxide was blocked with 3 % H_2O_2 for 10 min. After PBS washes, slides were blocked with 5 % normal goat serum in PBS for 15 min at room temperature followed by incubation with primary anti-STAT3 (1: 100), anti-VEGF (1: 500), anti-PCNA (1: 400) or anti-CD31 (1: 400) antibody in blocking solution overnight at 4 °C. All slides were subsequently incubated with a 1: 200 dilution of biotin-conjugated goat anti-mouse, goat anti-rat or goat anti-rabbit secondary antibody for 15 min at 37°C and streptavidin–biotin complex at 37°C for 15 min. The immunoreaction was visualized by using diaminobenzidine (DAB) peroxide solution and cellular nuclei were counterstained with hematoxylin. All specimens were evaluated using Olympus B×600 microscope and Spot Fiex camera. Control samples exposed to secondary antibody alone showed no specific staining.

To detect apoptotic cells in tumor tissues, TUNEL assay using a DeadEndTM Fluorometric TUNEL System (Promega, Madison, Wisc, USA) was performed following the manufacturer's protocol. Cell nuclei with dark green fluorescent staining were defined as TUNEL-positive nuclei. TUNEL-positive nuclei were monitored by fluorescence microscope. To quantify TUNEL-positive cells, the number of green fluorescence-positive cells was counted in random fields at × 200 magnification. Cell nuclei were counterstained with 4, 6-diamidino-2-phenylindole (DAPI).

Statistical analysis. Data are expressed as the mean ± SD. Statistical analysis was performed by Student's test for comparing two groups and by ANOVA for multiple group comparisons. $P<0.05$ was considered statistically significant. The Statistics Analysis System was used for all statistical analyses.

Results

Specific knockdown of STAT3 in 4T1 breast cancer cells in vitro. The pSi-STAT3 and pSi-Scramble plasmid were transfected into 4T1 breast cancer cells, respectively. Forty-eight hours later, the cells were harvested, and the expression level of STAT3 was analyzed by Western blot. As shown in Fig. 1A, dramatic suppression of STAT3 expression was observed in 4T1 cells treated with pSi-STAT3 plasmid, compared with blank group.

Then, the effect of Stat3 protein reduction on 4T1 cell proliferation was examined by MTT assay. We determined the absorbance at 0 h, 24 h, 48 h and 72h after 4T1 cells transfected with pSi-STAT3 plasmid. As shown in Fig 1B, there was no change in cell proliferation after the STAT3 knockdown in 4T1 cells ($p=0.71$). To further investigate the signaling pathway, we examined the upstream regulator and downstream targets of Stat3 in 4T1 cells after knockdown of STAT3. We found that the expression level of VEGF, MMP-9 and MMP-2 was reduced by pSi-STAT3 plasmid. At the same time, the phosphorylation of Src, the upstream regulator of Stat3, was eliminated in 4T1 cells after knockdown of STAT3, compared with the two control groups. However, there was no change in Src protein, as shown in Fig. 1C. To investigate the molecule mechanism of STAT3 on

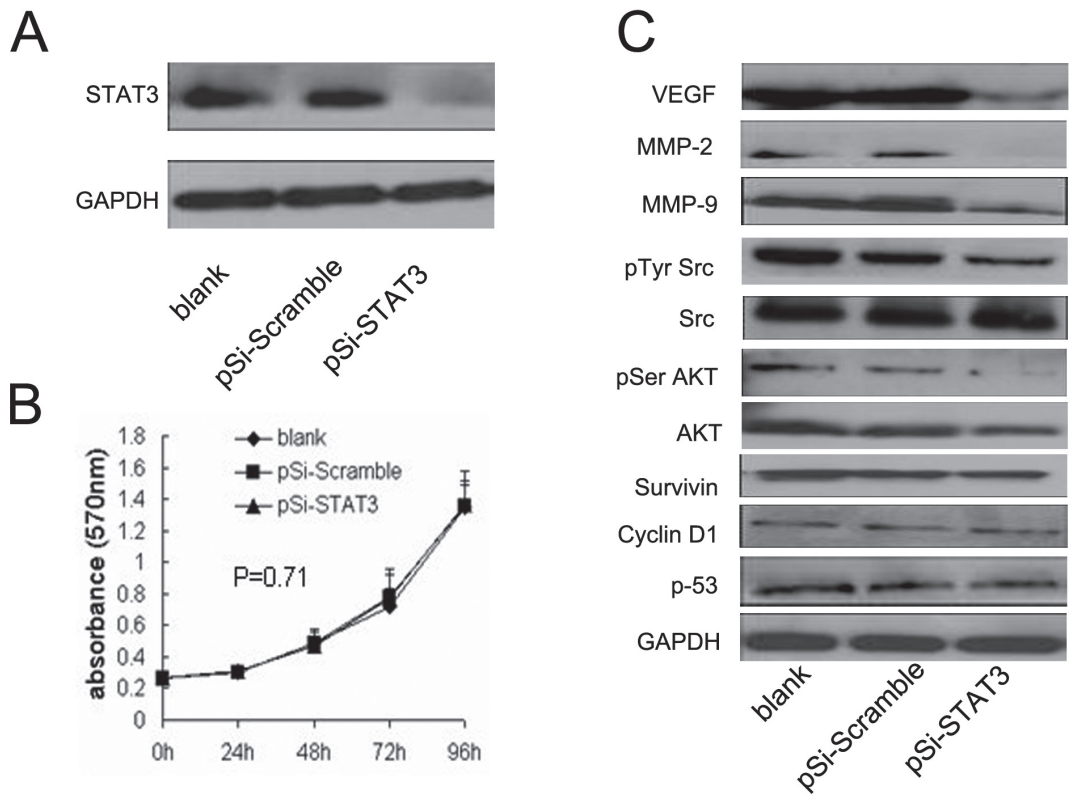

Figure 1. STAT3 knockdown in breast cancer 4T1 cells. A, forty-eight hours after 4T1 cells transfected with pSi-STAT3, Western blot was conducted on cell lysates with antibodies to Stat3 and GAPDH as a loading control. Equal amount of protein was loaded on each gel lane. B, the cell proliferation of 4T1 cells after STAT3 knockdown was determined by MTT assay. In this analysis, we examined the absorbance at 570 nm after 4T1 cells transfected with pSi-STAT3 plasmid for 0 h, 24 h, 48 h and 72 h. Cells were analyzed for each sample in triplicate. C, the effects of STAT3 knockdown in 4T1 cells on the upstream regulator and downstream targets. Western blot was conducted for the indicated protein in either 4T1 cells or transfected with pSi-Scramble and pSi-STAT3 plasmid. Equal amount of protein was loaded on each gel lane.

4T1 cell proliferation, we also examined the expression level of p53, Cyclin D1 and Survivin protein after STAT3 knockdown. As shown in Fig. 1C, no change was found in the p53, Cyclin D1 and Survivin protein level. In addition, the phosphorylation of Akt was reduced after STAT3 knockdown in 4T1 cells and the Akt protein level was not changed (Fig. 1C).

STAT3-siRNA inhibited HUVECs capillary-like structures formed in vitro. Tube formation, an assay for the capillary formation of HUVECs, is a simple but powerful tool for examining angiogenetic associations. In this study, after polymerizing the matrix at 37 °C, HUVECs were seeded onto the polymerized EC matrix at a concentration of 2×10^4 cells in 100 µl of EGM-2 media per well; 100 µl of the cell supernatant after transfected with pSi-STAT3 or pSi-Scramble 48 h was immediately added. After incubated at 37 °C for 6 h, HUVECs were grown to form capillary-like structures on the Matrigel™ surface in the blank and pSi-Scramble group, but the supernatant of pSi-STAT3 group inhibited the capillary-like structures formed (Fig. 2A). HUVECs capillary-like structures were counted as described in the "Materials and methods". The number of pSi-STAT3 group was significantly lower than that of the blank and pSi-Scramble group: 15.70± 1.60(pSi-STAT3) versus 42.90±0.90 (pSi-Scramble) and 46.60±2.20 (5% glucose, $p<1x10^{-4}$, Fig. 2B).

STAT3-siRNA inhibited 4T1 cells migration in vitro. The wound-healing assay was performed to determine the STAT3-siRNA effect on 4T1 cells migration. As shown in Fig. 2C, the results revealed that cell migration was inhibited in the pSi-STAT3 group, but no inhibition was observed in the two control groups, blank and pSi-Scramble. Image J software was used to calculate the migration rate (% of control, $P=1x10^{-4}$, Fig. 2D).

STAT3-siRNA inhibited 4T1 tumor growth and lung metastasis in vivo. We determined the effects of silencing STAT3 by plasmid-based siRNA on tumor growth and lung metastasis *in vivo*. 4T1 breast subcutaneous mice model was used in this study. Since the high capacity of migration and invasion, 4T1 cells could metastasize to the lung from primary tumor. So, it is the best mice model to investigate the effect on primary tumor growth and metastasis. As shown in Fig. 4A, treatment with pSi-STAT3/liposome complex statistically inhibited the primary 4T1 tumor growth in mice. At the end

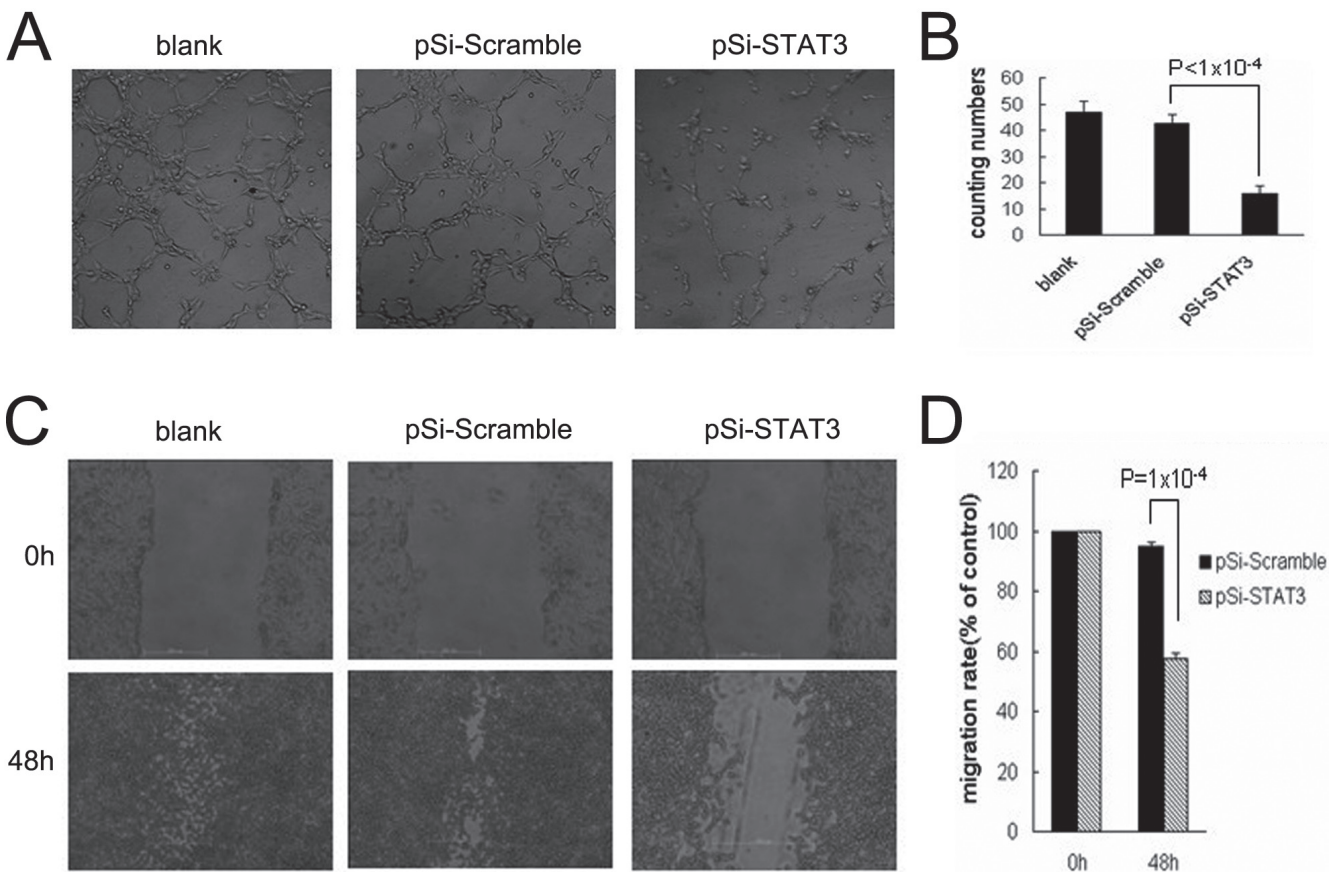

Figure 2. STAT3-siRNA inhibited 4T1 cell migration and HUVECs tube formation. A, effect of pSi-STAT3 on HUVECs tube formation *in vitro*. HUVECs were grown to form capillary-like structures in the left two pictures, and the tube was inhibited in the pSi-STAT3 group. Original magnification ×100. B, the HUVECs capillary-like structures were counted in per yield. Data were expressed as means ±SD (for each group, n=3). The experiment was performed in triplicate. C, the ability of 4T1 cells migration was determined by wound-healing assay *in vitro*. Scale was 200 μm. D, the percent of migrated cells was determined as described in the "Materials and Methods". Data were expressed as means ±SD (for each group, n=3). The experiment was performed in triplicate.

of treatment, pSi-STAT3 plasmids/liposome complex reduced tumor volume to 32.42 % of tumor volume from mice injected with pSi-Scramble plasmids/liposome complex ($p=2x10^{-4}$) and 28.56 % of tumor volume from mice injected with 5 % glucose (Fig. 3A). Moreover, tumor weight was measured at the termination of the animal experiment. Mean tumor weight was 0.37±0.11; 1.09±0.21; 1.15±0.31 in pSi-STAT3/liposome complex group, pSi-Scramble/liposome complex group and 5 % glucose group, respectively (p=0.008, Fig. 3B). Meanwhile, an 86.81 % decrease in the number of macroscopically visible lung metastases was achieved by pSi-STAT3/liposome complex ($p=2x10^{-4}$), compared with pSi-Scramble/liposome complex group. Examination of the lungs revealed an average of 4 visible lesions in mice injected with pSi-STAT3/liposome complex, whereas the 5 % glucose and pSi-Scramble/liposome complex group exhibited an average of 31 and 20 lung metastases, respectively (Fig. 3C&D). Furthermore, lung metastases were determined by H&E staining of the lung. As shown in Fig. 3E, fewer and smaller lung metastases were observed in the lung from pSi-STAT3/liposome complex treated mice than the two control groups.

STAT3-siRNA inhibited STAT3 and VEGF expression in vivo. To determine the STAT3 status in these tumors, we used immunohistochemistry to evaluate the level of STAT3 gene expression in tumor tissues. As shown in Fig. 4A, we got the results that STAT3 expression was inhibited in the mice treated with pSi-STAT3/liposome complex. VEGF take an important role in angiogenesis *in vivo*, and we have demonstrated that pSi-STAT3 significantly decreased the VEGF expression *in vitro*. Thus, immunohistochemistry was used to evaluate the expression level of VEGF in the tumor tissues. The results also suggested that VEGF expression was inhibited by the pSi-STAT3/liposome complex *in vivo*.

STAT3-siRNA inhibited angiogenesis in vivo. Angiogenesis in tumor tissues was assessed by immunohistochemistry by use of CD31 antibody, with high specific affinity for vascular endothelial cells. Brown staining by biotinylation was observed by microscopy. Our data suggested that the mean

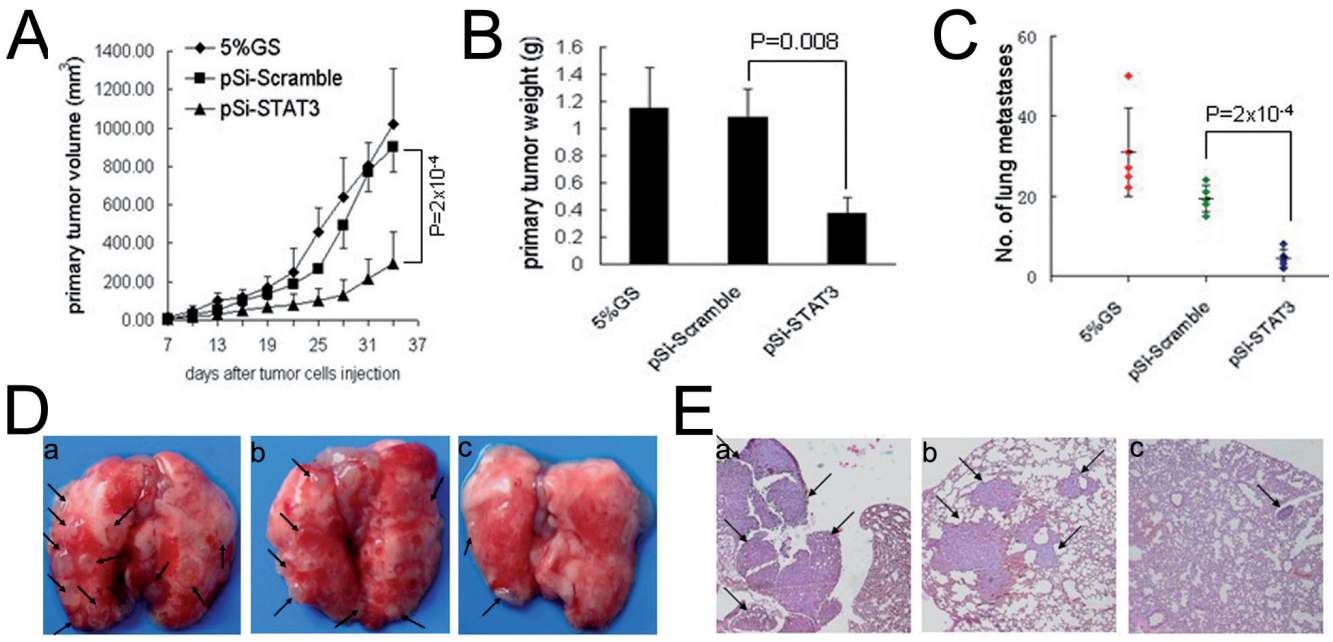

Figure 3. Anti tumor efficacy of pSi-STAT3. A, seven days after tumor cell injection, mice were randomly assigned to one of three groups and treated as follows: (a) 5% glucose solution; (b) pSi-Scramble and (c) pSi-STAT3. Tumor volume was recorded during the treatment. B, mice were euthanized after 10 times of treatment and dissected tumors were weighed (for each group, n=5). C, number of visible lung metastases in 4T1 tumor-bearing mice treated with pSi-STAT3 /liposome complex or the two control groups. Data were expressed as means ±SD (for each group, n=5). D&E, brightfield imaging of the lungs from 4T1 tumor-beating mice treated with 5% glucose solution (a); pSi-Scramble/liposome complex (b) and pSi-STAT3 /liposome complex (c). H&E staining was used to test the metastases of the lungs. Fewer lung metastases were found in the pSi-STAT3/liposome complex group. Arrows indicated the lung metastases.

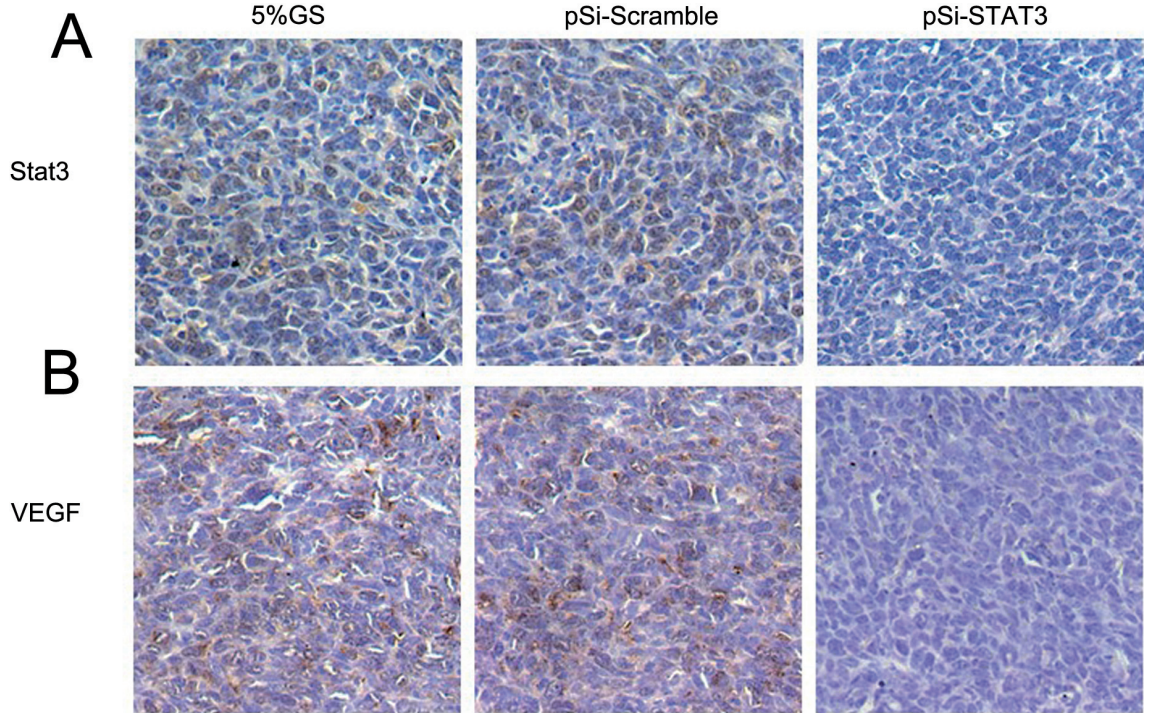

Figure 4. Silencing of STAT3 and VEGF expression by pSi-STAT3 *in vivo*. A, tumor tissues from tumor-bearing mice treated with pSi-STAT3/liposome complex or pSi-Scramble / liposome complex or 5% glucose were immunostained with Stat3. Original magnification × 400. B, to evaluate the expression level of VEGF *in vivo*, tumor tissues from tumor-bearing mice treated with pSi-STAT3/liposome complex or pSi-Scramble / liposome complex or 5% glucose were used to immunostaining. Original magnification × 400.

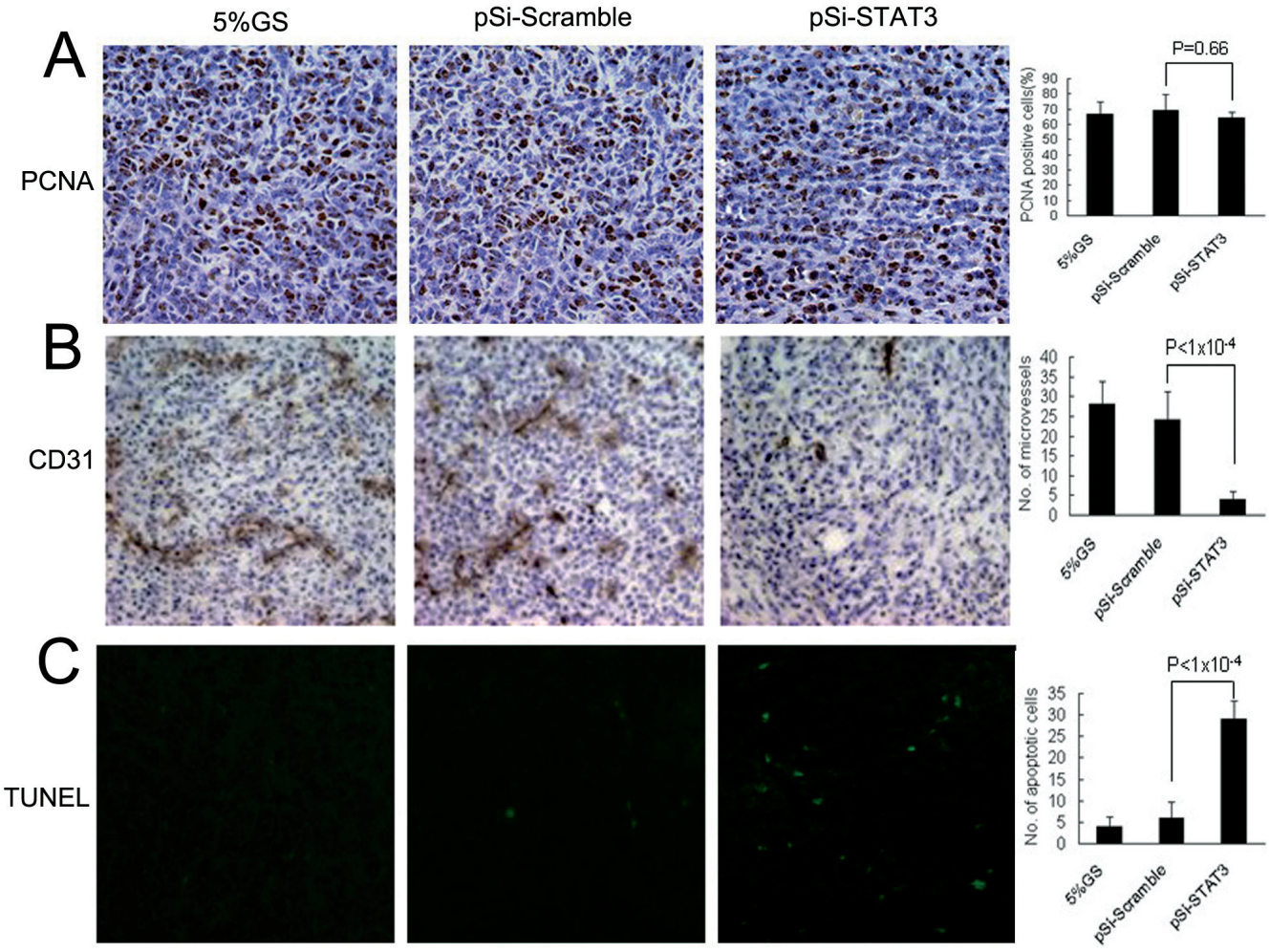

Figure 5. Effects of pSi-STAT3 on cell proliferation, angiogenesis and apoptosis *in vivo*. A, percentages of PCNA-positive nuclei showed no statistical difference among the three groups (p>0.05). Original magnification ×400. B, the MVD in pSi-STAT3 / liposome complex group was significantly lower than that in the two control group. Original magnification ×400. C, TUNEL assay showed that the TUNEL-positive nuclei significantly increase in pSi-STAT3 / liposome complex group compared with 5 % glucose and pSi-Scramble / liposome complex group. Original magnification ×200.

microvascular density (MVD) was dramatically lower in the tumors treated with pSi-STAT3/liposome complex than in the two control groups: 4.30±0.97 (pSi-STAT3/liposome complex) versus 24.60±1.80 (pSi-Scramble/liposome complex; $p<1x10^{-4}$) and 28.20±3.21 (5 % glucose, Fig. 5B). Meanwhile, no significant difference of mean MVD was found between the control groups (p>0.05).

STAT3-siRNA induced tumor apoptosis in vivo. The TUNEL assay was applied to detect apoptosis in tumor tissues. As shown in Fig. 5C, within a similar field of view, more TUNEL-positive cells were observed in tumor tissues from the mice treated with pSi-STAT3/liposome complex than pSi-Scramble/liposome complex and 5 % glucose: 29.60±3.40 versus 6.20±1.90 or 4.10±0.80 ($p<1x10^{-4}$). Cell nuclei were counterstained with 4, 6-diamidino-2-phenylindole (DAPI), data not shown. In addition, we performed PCNA immunostaining to further study the STAT3-siRNA effect on tumor cell proliferation. According to the data, the percentage of PCNA-positive cells was 66.5±8.1 %, 69.3±10.6 % and 64.0±4.3 % in 5 % glucose, pSi-Scramble/liposome complex and pSi-STAT3/liposome complex, respectively (p=0.66, Fig. 5A).

Discussion

In the present study, we used a 4T1 breast cancer model that could form metastases in the lung to evaluate whether knockdown of STAT3 by systemic delivery of pSi-STAT3 inhibits primary tumor growth and metastasis. Our results show that pSi-STAT3 leads to a significant inhibition of tumor growth and metastasis mediated by inducing tumor cell apoptosis, reducing angiogenesis and inhibiting cell invasion.

As a primary tumor grows, it needs to develop a blood supply that can support its metabolic needs – a process called angiogenesis. Meanwhile, these new blood vessels can also provide an escape route by which cells can leave the tumor and enter into the body's circulatory blood system (18). Continued tumor growth at metastatic sites is angiogenesis dependent too (19). Angiogenesis is a complicated process that tightly regulated by both positive and negative regulators, most important is VEGF. Thus VEGF-targeting is the most useful strategy for cancer gene therapy. Granulocyte macrophage colony-stimulating factor (GM-CSF) was used to inhibit breast cancer growth and metastasis by blocking VEGF activity (20). Xie *et al* have reported that VEGF is down regulated by knockdown of STAT3 in melanoma cells (5). In our study, we found that the expression of VEGF in 4T1 breast cancer cells was reduced by pSi-STAT3 *in vitro* and *in vivo*. Further results showed that pSi-STAT3 reduced blood vessels formation significantly ($p<1x10^{-4}$) in tumor tissues. Since cutting down the support of metabolic needs of solid tumor, tumor cell apoptosis induction ($p<1x10^{-4}$) and lung metastases inhibition ($p=2x10^{-4}$) were found in the pSi-STAT3 group. These results correlate well with other studies examining the biological effects of VEGF blockade in patients treated with Bevacizumab (Avastin) (21).

As a point of convergence for various oncogenic signaling pathways, STAT3 regulates numerous oncogene and cancer suppressor gene expressions. Activated STAT3 can induce NF-κB p100 processing to P52, which subsequently inhibits the apoptosis of prostate cancer cells (22). STAT3 also can repress p53 expression by binding to the p53 promoter and affect p53-mediated tumor cell apoptosis (23). Recent studies have shown that STAT3 activation is required for the induction of MMP-9 in transformed human mammary epithelial cells (24). Twist, inducing tumor metastasis by silencing E-cadherin expression and EMT induction, has been found that takes an important role in breast cancer metastasis (8, 25). Therapeutic silencing of miR-10b, which is a downstream target of Twist, inhibits metastasis to lungs in 4T1 mammary mouse model (26). Importantly, in our study, we found that knockdown of STAT3 by pSi-STAT3 inhibits MMP-2 and MMP-9 protein expression (Fig. 1C) and Twist mRNA expression (data not shown) in 4T1 cells. The inhibition of MMP-2, MMP-9 and Twist expression is consistent with our findings that 4T1 cells treated with pSi-STAT3 lose the ability to migrate *in vitro* ($p=1x10^{-4}$) and metastasize to lung from primary tumor *in vivo* ($p=2x10^{-4}$).

Additionally, activated STAT3 has been shown to protect tumor cells from apoptosis and promote cell proliferation by regulating genes encoding antiapoptotic and proliferation-associated proteins, such as Bcl-xL, Mcl-1, Bcl-2, Fas, cyclin D1, and c-Myc (27-30). Interestingly, we found that the proliferation and apoptosis of 4T1 cells transfected with pSi-STAT3 *in vitro* were not significantly different from the pSi-Scramble and blank groups, whereas pSi-STAT3 significantly induced tumor cell apoptosis in 4T1 tumor model. The mechanism of VEGF inducing apoptosis may explain the different results we got. It's well known that growth, persistence and dissemination of solid tumors are angiogenesis dependent (31). The tumor will lose their support of metabolic needs after knockdown of VEGF, because blood vessels are inhibited. This would induce tumor cell apoptosis *in vivo*. Whereas, i*n vitro*, the blood vessels are not necessary for cells getting metabolic needs. At the same time, Twist is not required for the proliferation of 4T1 cells in culture (8). There are various evidences that altered STAT3 activity may inhibit proliferation in cancer cells. However, it's interesting to note that pSi-STAT3 had no effect on 4T1 cells proliferation *in vitro* and *in vivo*, suggesting different molecular bases for cell proliferation exit in different cell lines. To further investigate the difference of molecular bases between 4T1 cells and the others, we examined the expression level of p53, Cyclin D1 and Survivin, which take an important role in cell proliferation or apoptosis and were reduced after knockdown of STAT3 in ovarian cancer and other breast cancer (32, 33). No change was found among the p53, Cyclin D1 and Survivin protein level. These results correlate well with the effect of STAT3 on the cell proliferation of 4T1 cells.

Gene therapy is a potential strategy for curing cancer and other diseases, but its success is highly dependent on delivery and expression system. Currently, gene therapy delivery system can be generally categorized into virus-based and nonvirus-based vectors. Viral vectors are highly efficient, but the safety is concerned due to their oncogenic potential, inflammatory and immunogenic effects (34). By contrast, nonviral vectors, such as liposomes take the advantages of less immunogenic and toxic, easy for large-scale production and there is no limitation on the size of transferred DNA theoretically (35,36). At present, cationic liposome is the most extensively investigated vector and has been successfully used to deliver genes, proteins, oligonucleotides and antibiotics in several cell types (37-39). In our lab, we used DOTAP-cholesterol liposome as the vector deliver system and demonstrated that it gets the advantage of highly efficient *in vitro* and *in vivo* (40, 41). RNAi is the efficient way to regulate the expression of protein-coding genes (11). Following the initial reports, it takes a remarkable short period of time for siRNAs triggers to be adopted as a standard component of the molecular biology toolkit (13). Compared with chemically synthesized siRNA, plasmid-based siRNA expression system can potentially mediate long-term silencing with a single application (42). Besides, shRNA is less likely to induce specific and non-specific off-target effects, because it is spliced by endogenous mechanisms (43). Therefore, pGenesil-2 plasmid vector was used to express small interfering RNA targeting STAT3 in our study. The results indicated that pSi-STAT3 significantly inhibits 4T1 tumor growth and metastasis by systematic administration with DOTAP-cholesterol liposomes. In the present study, we didn't find any side effects in animals.

Metastases are the major cause of cancer-related mortality (2). For the advancing in the past decades, there are still several clinical challenges for curing tumor metastases (1).

The metastatic process consists of a series of steps: invasion, which initiates the metastatic process; survival and arrest in the bloodstream and metastatic colonization that the final steps in the metastatic process, outgrowth at a distant site. In our study, blocking VEGF activity through pSi-STAT3 resulted in angiogenesis and primary tumor growth inhibition. Since blood vessels were inhibited, the tumor cells lost the route to metastasis. Importantly, VEGF is not the only target of STAT3 in 4T1 cells, MMP-2, MMP-9 and Twist are also regulated by STAT3. Knockdown of MMP-2, MMP-9 and Twist caused the 4T1 cell losing the ability of migration *in vitro* and invasion *in vivo*. Thus, STAT3-siRNA gets the double effect on inhibiting tumor cell metastasis: cutting down the escape route and destroying the microenvironment of cell invasion. According to the "seed and soil" theory first published in 1889 by Stephen Paget (44), further studies should be taken to investigate whether STAT3-siRNA destroy the soil-lung microenvironment. Maybe it take an important role in inhibiting lung metastases formed.

In summary, we have shown that plasmid-based STAT3-siRNA expression system can efficiently inhibit STAT3, VEGF, MMP-2 and MMP-9 expression *in vitro* and systematic delivery of pSi-STAT3 by cationic liposomes leading to increased apoptosis, decreased tumor vascularity and lung metastases *in vivo*. These results indicate that targeting STAT3 with plasmid-based siRNA may have therapeutic benefit in the treatment of breast primary as well as metastatic tumor.

Acknowledgments: This work is supported by Hi-tech Research and Development Program (863 Program) of China (2007AA021008 and 2009ZX09102-241). The National Key Basic Research Program (973 Program) of China (2010CB529900).

References

[1] STEEG PS. Tumor metastasis: mechanistic insights and clinical challenges. Nat Med 2006;12: 895-904.

[2] FIDLER IJ. The pathogenesis of cancer metastasis: the 'seed and soil' hypothesis revisited. Nat Rev Cancer 2003; 3: 453-458. doi:10.1038/nrc1098

[3] KAMANGAR F, DORES GM and ANDERSON WF. Patterns of cancer incidence, mortality, and prevalence across five continents: defining priorities to reduce cancer disparities in different geographic regions of the world. J Clin Oncol 2006; 24: 2137-2150. doi:10.1200/JCO.2005.05.2308

[4] GARCIA R, YU CL, HUDNALL A, CATLETT R, NELSON KL et al. Constitutive activation of Stat3 in fibroblasts transformed by diverse oncoproteins and in breast carcinoma cells. Cell Growth Differ 1997; 8: 1267-1276.

[5] XIE TX, HUANG FJ, ALDAPE KD, KANG SH, LIU M et al. Activation of stat3 in human melanoma promotes brain metastasis. Cancer Res 2006; 66: 3188-3196. doi:10.1158/0008-5472.CAN-05-2674

[6] STETLER-STEVENSON WG, HEWITT R AND CORCORAN M. Matrix metalloproteinases and tumor invasion: from correlation and causality to the clinic. Semin Cancer Biol 1996; 7: 147-154. doi:10.1006/scbi.1996.0020

[7] CHENG GZ, ZHANG WZ, SUN M, WANG Q, COPPOLA D et al. Twist is transcriptionally induced by activation of STAT3 and mediates STAT3 oncogenic function. J Biol Chem 2008; 283: 14665-14673. doi:10.1074/jbc.M707429200

[8] YANG J, MANI SA, DONAHER JL, RAMASWAMY S, ITZYKSON RA et al. Twist, a master regulator of morphogenesis, plays an essential role in tumor metastasis. Cell 2004; 117: 927-939. doi:10.1016/j.cell.2004.06.006

[9] DEO DD, AXELRAD TW, ROBERT EG, MARCHESILI V, BAZAN NG et al. Phosphorylation of STAT-3 in response to basic fibroblast growth factor occurs through a mechanism involving platelet-activating factor, JAK-2, and Src in human umbilical vein endothelial cells. Evidence for a dual kinase mechanism. J Biol Chem 2002; 277: 21237-21245. doi:10.1074/jbc.M110955200

[10] SCHAEFER LK, REN Z, FULLER GN AND SCHAEFER TS. Constitutive activation of Stat3alpha in brain tumors: localization to tumor endothelial cells and activation by the endothelial tyrosine kinase receptor (VEGFR-2). Oncogene 2002; 21: 2058-2065. doi:10.1038/sj.onc.1205263

[11] HANNON GJ. RNA interference. Nature 2002; 418: 244-251. doi:10.1038/418244a

[12] PAI SI, LIN YY, MACAES B, MENESHIAN A, HUNG CF et al. Prospects of RNA interference Therapy for cancer. Gene Ther 2006; 13: 464-477. doi:10.1038/sj.gt.3302694

[13] HANNON GJ AND ROSSI JJ. Unlocking the potential of the human genome with RNA interference. Nature 2004; 431: 371-378. doi:10.1038/nature02870

[14] PULASKI BA, TERMAN DS, KHAN S, MULLER E and OSTRAND-ROSENBERG S. Cooperativity of staphylococcal aureus enterotoxin B superantigen, major histocompatibility complex class II, and CD80 for immunotherapy of advanced spontaneous metastases in a clinically relevant postoperative mouse breast cancer model. Cancer Res 2000; 60: 2710-2715.

[15] CRONIN PA, WANG JH and REDMOND HP. Hypoxia increases the metastatic ability of breast cancer cells via upregulation of CXCR4. BMC Cancer 2010; 10: 225. doi:10.1186/1471-2407-10-225

[16] WALSH C, TANJONI I, URYU S, TOMAR A, NAM JO et al. Oral delivery of PND-1186 FAK inhibitor decreases tumor growth and spontaneous breast to lung metastasis in pre-clinical models. Cancer Biol Ther 2010; 9: 778-790. doi:10.4161/cbt.9.10.11433

[17] KORTYLEWSKI M, SWIDERSKI P, HERRMANN A, WANG L, KOWOLIK C et al. In vivo delivery of siRNA to immune cells by conjugation to a TLR7 agonist enhances antitumor immune responses. Nat Biotechnol 2009; 27: 925-932. doi:10.1038/nbt.1564

[18] WYCKOFF JB, JONES JG, CONDEELIS JS AND SEGALL JE. A critical step in metastasis: in vivo analysis of intravasation at the primary tumor. Cancer Res 2000; 60: 2504–2511.

[19] CHAMBERS AF, GROOM AC and MACDONALD IC. Dissemination and growth of cancer cells in metastatic sites. Nature Rev Cancer 2002; 2: 563-572. doi:10.1038/nrc865

[20] EUBANK TD, ROBERTS RD, KHAN M, CURRY JM, NUOVO GJ et al. Granulocyte macrophage colony-stimulating factor

inhibits breast cancer growth and metastasis by invoking an anti-angiogenic program in tumor-educated macrophages. Cancer Res 2009; 69: 2133-2140. doi:10.1158/0008-5472.CAN-08-1405

[21] BURSTEIN HJ, CHEN YH, PARKER LM, SAVOIE J, YOUNGER J et al. VEGF as a marker for outcome among advanced breast cancer patients receiving anti-VEGF therapy with bevacizumab and vinorelbine. Clin Cancer Res 2008; 14: 7871-7877. doi:10.1158/1078-0432.CCR-08-0593

[22] NADIMINTY N, LOU W, LEE SO, LIN X, TRUMP DL et al.Stat3 activation of NF-{kappa}B p100 processing involves CBP/p300-mediated acetylation. Proc Natl Acad Sci USA 2006; 103: 7264-7269. doi:10.1073/pnas.0509808103

[23] NIU G., WRIGHT KL, MA Y, WRIGHT GM, HUANG M et al. Role of Stat3 in regulating p53 expression and function. Mol Cell Biol 2005; 25: 7432-7440. doi:10.1128/MCB.25.17.7432-7440.2005

[24] DECHOW TN, PEDRANZINI L, LEITCH A, LESLIE K, GERALD WL et al. Requirement of matrix metalloproteinase-9 for the transformation of human mammary epithelial cells by Stat3-C. Proc Natl Acad Sci USA 2004; 101: 10602-10607. doi:10.1073/pnas.0404100101

[25] VERNON AE and LABONNE C. Tumor metastasis: A new Twist on epithelial mesenchymal transitions. Curr Biol 2004; 14: R719-R721. doi:10.1016/j.cub.2004.08.048

[26] MA L, REINHARDT F, PAN E, SOUTSCHED J, BHAT B et al. Therapeutic silencing of mir-10b inhibits metastasis in a mouse mammary tumor model. Nature Biotechnol 2010; 28: 341-347. doi:10.1038/nbt.1618

[27] CATLETT-FALCONE R, LANDOWSKI TH, OSHIRO MM, TURKSON J, LEVITZKI A et al. Constitutive activation of Stat3 signaling confers resistance to apoptosis in human U266 myeloma cells. Immunity 1999; 10: 105-115. doi:10.1016/S1074-7613(00)80011-4

[28] NIU, G, HELLER R, CATLETT-FALCONE R, COPPOLA D, JAROSZESKI M et al. Gene therapy with dominant–negative Stat3 suppresses growth of the murine melanoma B16 tumor in vivo. Cancer Res 1999; 59: 5059-5063.

[29] BOWMAN T, BROOME MA, SINIBALDI D, WHARTON W, PLEDGER WJ et al. Stat3-mediated Myc expression is required for Src transfor-mation and PDGF-induced mitogenesis. Proc Natl Acad Sci USA 2001; 98: 7319–7324. doi:10.1073/pnas.131568898

[30] BROMBERG JF, WRZESZCZYNSKA MH, DEVGAN G, ZHAO Y, PESTELL RG et al. Stat3 as an oncogene. Cell 1999; 98: 295-303. doi:10.1016/S0092-8674(00)81959-5

[31] FOLKMAN J. Role of angiogenesis in tumor growth and metastasis. Semin Oncol 2002; 29(6 Suppl 16): 15-18. doi:10.1016/S0093-7754(02)70065-1

[32] HUANG F, TONG XY, FU LQ AND ZHANG RH. Knockdown of STAT3 by shRNA inhibits the growth of CAOV3 ovarian cancer cell line in vitro and in vivo. Acta Biochim Biophys Sin 2008; 519-525. doi:10.1111/j.1745-7270.2008.00424.x

[33] GRITSKO T, WILLIAMS, TURKSON J, KANEKO S, BOWMAN T et al. Persistent activation of stat3 signaling induces surviving gene expression and confers resistance to apoptosis in human breast cancer cells. Clin Cancer Res 2006; 12:11-19. doi:10.1158/1078-0432.CCR-04-1752

[34] GUO Y, GUO H, ZHANG L, XIE H, ZHAO X et al. Genomic analysis of anti-hepatitis B virus activity by small interfering RNA and lamivudine in stable HBV-producing cells. Journal of Virology 2005; 79: 14392-14403. doi:10.1128/JVI.79.22.14392-14403.2005

[35] ZHDANOV RI, PODOBED OV AND VLASSOV VV. Cationic liposome-DNA complexes-lipoplexes-forgene transfer and therapy. Bioelectrochemistry 2002; 58: 53-64. doi:10.1016/S1567-5394(02)00132-9

[36] YOUNG LS AND MAUTNER V. The promise and potential hazards of adenovirus gene therapy. Gut 2001; 48 733-736. doi:10.1136/gut.48.5.733

[37] JIAO X, WANG RY, QIU Q, ALTER HJ and SHIH JW. Enhanced hepatitis C virus NS3 specific Th1 immune responses induced by co-delivery of protein antigen and CpG with cationic liposomes. J Gen Virol 2004; 85(Pt 6): 1545-1553. doi:10.1099/vir.0.79896-0

[38] ZELPHATI O and SZOKA FC Jr. Mechanism of oligonucleotide release from cationic liposomes. Proc Natl Acad Sci USA 1996; 93: 11493-11498. doi:10.1073/pnas.93.21.11493

[39] SANGARE L, MORISSET R, OMRI A and RAVAOARINORO M. Incorporation rates, stabilities, cytotoxicities and release of liposomal tetracycline and doxycycline in human serum. J Antimicrob Chemother 1998; 42: 831-834. doi:10.1093/jac/42.6.831

[40] YANG Y, BAI Y, XIE G, ZHANG N, MA YP et al. Efficient inhibition of non-small cell lung Cancer xenograft by systemic delivery of plasmid encoding short hairpin RNA targeting VEGF. Cancer Biotherapy & Radiopharmaceuticals 2010; 25: 65-73. doi:10.1089/cbr.2009.0692

[41] WAN Y, HUANG AL, YANG Y, XIE G, CHEN X et al. A vector-based short hairpin RNA targeting Aurora A inhibits breast cancer growth. International Journal of Oncology 2010; 36: 1121-1128.

[42] DUCHAINE TF and SLACK FJ. RNA interference and micro-RNA–oriented therapy in cancer: rationales, promises, and challenges. Curr Oncol 2009; 16: 61-66. doi:10.3747/co.v16i4.486

[43] RAO DD, VORHIES JS, SENZER N and NEMUNAITIS J. siRNA vs. shRNA: similarities and differences. Adv Drug Deliv Rev 2009; 61:746-759. doi:10.1016/j.addr.2009.04.004

[44] PAGET S. The distribution of secondary growths in cancer of the breast. Lancet 1889; 133: 571-573. doi:10.1016/S0140-6736(00)49915-0